LBL-24941

Lawrence Berkeley Laboratory
UNIVERSITY OF CALIFORNIA

OCCUPATIONAL HEALTH DIVISION

CONF-880404--6

To be presented at the Seventh International Congress
of the International Radiation Protection Association,
Sydney, Australia, April 10–17, 1988

Field Characterization and Personal Dosimetry at a High Energy Ion Accelerator

N.A. Greenhouse, D.D. Busick, T.M. de Castro, A.J. Elwyn,
D.E. Hankins, N.E. Ipe, P.R. La Plant, J.B. McCaslin,
T.R. Renner, A.R. Smith, R.-K.S. Sun, and W.P. Swanson

March 1988

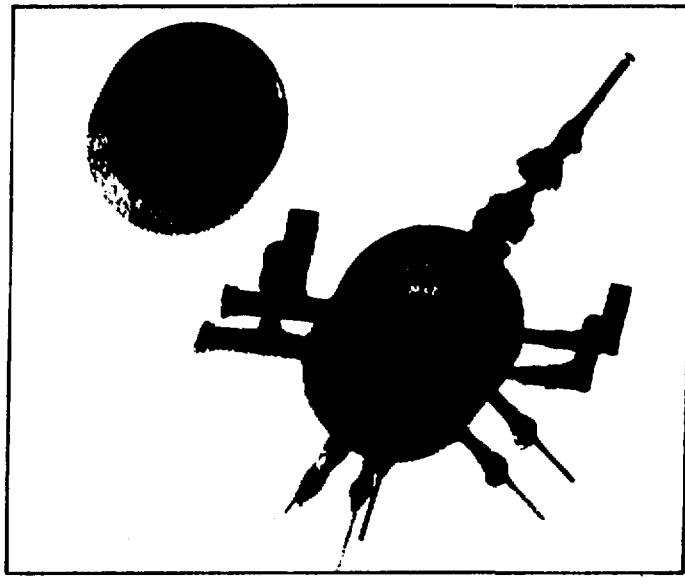

Prepared for the U.S. Department of Energy under Contract DE-AC03-76SF00098

LBL--24941

DE88 008208

FIELD CHARACTERIZATION AND PERSONAL DOSIMETRY AT A HIGH ENERGY HEAVY ION ACCELERATOR

N. A. Greenhouse, D. D. Busick(a), T. M. de Castro, A. J. Elwyn(b), D. E. Hankins(c), N. E. Ipe(a), P. R. La Plant, J. B. McCaslin, T. R. Renner, A. R. Smith, R.-K. S. Sun and W. P. Swanson

Lawrence Berkeley Laboratory
University of California
Berkeley, CA 94720, USA
(a) Stanford Linear Accelerator Center, Stanford, CA 94305, USA
(b) Fermi National Accelerator Laboratory, Batavia, IL 60510, USA
(c) Lawrence Livermore National Laboratory, Livermore, CA 94550, USA

ABSTRACT

The response of a variety of dosimeters was evaluated in the radiation field outside the shielding of the Lawrence Berkeley Laboratory Bevalac Biomedical Facility. The primary beam was 580 MeV/A neon ions, incident upon a 30.5-cm polyethylene cube. The field was characterized by a neutron spectrometer consisting of Bonner spheres and other detectors and by estimates of charged particle fluences in NTA film and in the Berklet spectrometer. The responses of American Acrylics CR-39 track-etch plastic detectors and AECL (Canada) type BD-100 Bubble Detectors were compared to those of NTA film, Andersson-Braun remmeter and recombination-chamber results as well as to reference dose equivalents based upon the unfolded neutron spectrum. Evaluations of these dosimeters are discussed.

March 3, 1988

FIELD CHARACTERIZATION AND PERSONAL DOSIMETRY AT A HIGH ENERGY HEAVY ION ACCELERATOR

N. A. Greenhouse, D. D. Busick[a], T. M. de Castro, A. J. Elwyn[b], D. E. Hankins[c], N. E. Ipe[a], P. R. La Plant, J. B. McCaslin, T. R. Renner, A. R. Smith, R.-K. S. Sun and W. P. Swanson

Lawrence Berkeley Laboratory
University of California
Berkeley, CA 94720, USA
(a) Stanford Linear Accelerator Center, Stanford, CA 94305, USA
(b) Fermi National Accelerator Laboratory, Batavia, IL 60510, USA
(c) Lawrence Livermore National Laboratory, Livermore, CA 94550, USA

This experiment was designed, firstly, to characterize the complex radiation field outside the shielding of the Lawrence Berkeley Laboratory (LBL) Bevalac Biomedical Facility, and secondly, to evaluate a variety of detectors in such a field. In particular, the responses of American Acrylics CR-39 track-etch plastic and AECL (Canada) type BD-100 Bubble Detectors were compared to those of NTA film, rem-meter and recombination-chamber results as well as to reference dose equivalents based upon the unfolded neutron spectrum.

EXPERIMENTAL METHOD

The Biomedical Control Room at the LBL Bevalac heavy-ion accelerator was the site selected for this experiment (Fig. 1). Neon ions at 580 MeV·A were stopped in a 30.5-cm polyethylene cube at the patient isocenter. Detectors were placed on the opposite side of an 0.91-m thick concrete wall at about 90° to the beam direction. This location afforded an opportunity to study dosimeters in a mixed-hadron field extending to high energies. All data were normalized to primary beam current via a secondary emission monitor (SEM), for which an absolute calibration was made.

The neutron field was characterized by unfolding the spectrum from measurements taken with an array of seven Bonner spheres (diameters 0 to 0.305m) and $^{27}Al(n,\alpha)^{24}Na$ and $^{12}C(n,2n;\ p,pn)^{11}C$ activation detectors having thresholds of 6.5 and 20 MeV, respectively. In addition to spectral information, the unfolding code LOUHI78 [1], provided estimates of the average neutron quality factor (Q), absorbed dose (D) and dose equivalent (H). Independent assessments of Q and H were provided by a recombination chamber [2], an integrating Andersson-Braun rem meter, and a polyethylene-moderated BF_3 proportional counter calibrated with a standard $^{238}PuBe$ source.

Irradiations of neutron dosimeters were conducted under identical beam conditions. CR-39, BD-100 and NTA film dosimeters were irradiated on an anthropomorphic torso phantom (location A) where the neutron dose equivalent rate was about 200 μSv h^{-1} for a primary beam current of 2.5×10^{6} Ne s^{-1}. CR-39 and BD-100 dosimeters were also irradiated on an ANSI [3] neutron phantom 1 meter away at location B. This was an area of lower dose rate and somewhat softer spectrum.

The track etch dosimeters were processed by the electrochemical etching method of Hankins *et al.* [4] and scanned over a detector area of 0.54 cm^2. Dose equivalents are

based upon a calibration to 14 MeV neutrons of 2.31×10^{5} tracks cm^{-2} Sv^{-1}. The bubble detectors were processed according to the manufacturer's instructions. Sensitivities of the glass and plastic bubble detectors are 30 and 180 bubbles per μSv, respectively, for a PuBe spectrum. The NTA films were developed per the recommendations of Kodak the day following exposure, and evaluated using a 400-power dark-field scan for tracks over a 9.35×10^{-4} cm^{2} emulsion area (net track-density to dose conversion of 8.56×10^{5} tracks cm^{-2} Sv^{-1}).

Previous work suggested that charged particles exist near the phantom locations. This was confirmed by measurements made with the Berklet spectrometer [5] at locations shown in Fig. 1. Spectra are shown in Fig. 2 for proton energies above 16 MeV.

COMPARISON OF DOSIMETERS

Spectral data from the neutron spectrometer are shown in Figs. 3 and 4. The reference dose equivalents, H_{nf}, against which the doslmeter responses were compared were derived from the unfolding code, LOUHI78. Average quality factor estimates over all components of the radiation field from recombination-chamber measurements were 4.2 and 4.1 ($\pm$ 1.1) at dosimeter locations A and B, as compared with the estimates of neutron quality factor from the neutron spectrometer of 4.9 and 5.1, respectively.

Table 1 shows a comparison of four dosimeter responses with the neutron dose equivalents derived from the neutron spectrometer, H_{nf}. Three of the measurements (excepting the NTA film) are reasonably consistent among themselves but give lower responses than H_{nf}. In particular, the CR-39 and BD-100 dosimeters apparently underrespond by 30 to 40% and 30 to 60%, respectively. In contrast the NTA dosimeters, which respond to both protons and neutrons, greatly overestimate the dose equivalent, primarily because they register incident charged particles, with $\approx$100% efficiency.

Table 1. Comparison of dosimeter response to neutron spectrometer H_{nf}.
(Dose equivalent in mSv per 1×10^{13} Ne)

Location	H_{nf}, Neutron Spectrometer	A-B* Rem-meter	CR-39**	BD-100**	NTA Film
A	2.15	1.10	1.37±0.15	1.13±0.12(g) 0.95±0.11(p)	22.7
B	1.22	0.74	0.85±0.17	0.76±0.11(g) 0.85±0.31(p)	—

* Negligible statistical error. ** Uncertainties are standard errors from scanning multiple fields. (g) Glass BD-100 Bubble Detector (no longer available). (p) Plastic BD-100 Bubble Detector.

Evaluation of the NTA film revealed large numbers of charged particles that traversed the 30-μm layer of sensitive emulsion. The minimum proton energy required to traverse this thickness perpendicularly is about 1.7 MeV. The charged particle fluence above this energy, derived from counting tracks that penetrate the sensitive layer completely, is 3.5×10^{-9} cm^{-2} per primary Ne ion as compared to the total neutron fluence of 6.8×10^{-7} cm^{-2} Ne^{-1} (all energies). The Berklet detector (sensitive to protons > 16 MeV) measured charged particle spectra at three locations marked on Fig. 1. Figure 2 shows a decline of the number of such particles and an apparent flattening of the spectra with

increasing angle from the beam direction.

DISCUSSION

The experimental arrangement provides an opportunity to study dosimeter response in a field containing significant fluences of both high energy neutrons and protons. The spectrum for location A (Figs. 3, 4) is qualitatively typical of both dosimetry locations. The two peaks at about 0.1 and 10 MeV persisted throughout our attempts to refine the spectra. They are attributed to evaporation neutrons and to the transmission of higher energy neutrons through the thin shield. The minimum proton energy needed to traverse the concrete shield is about 650 MeV, but values as high as 2.9 GeV are kinematically possible at 90° for Ne-C interactions. The charged-particle field observed can therefore be tentatively ascribed in part to protons from the target that are transported directly through the shield.

The under-response of the plastic BD-100 dosimeters suggests a reduced sensitivity for the higher energy components in the neutron fields. These dosimeters should not respond to protons above ≈0.5 MeV because of decreasing LET [6], and therefore their response is mainly due to neutrons. An important result of this experiment was the rough correspondence between the CR-39 and the reference dose equivalents from the neutron spectrometer. However, the correspondence could result from the fortuitous response to incident charged particles. CR-39 has a limited energy range of response to protons, but probably greater than that of the BD-100 detectors [7]. The response of these two dosimeters is not well known but will be evaluated in future studies.

We attribute the excess response of the NTA film above the reference neutron dose to tracks from incident charged particles. This overestimate was noted for films attached to both the proximal and distal sides of the phantom, and suggests that these particles were sufficiently energetic to be transmitted by the phantom, or were produced by neutron interactions within it.

It is well known that radiation fields around high energy machines are complex. The authors wish to note the paramount importance of understanding these fields before dosimeter responses can be properly interpreted.

This work was supported by the U. S. Department of Energy under Contract No. DE-AC03-76SF00098 with the University of California.

REFERENCES

[1] J. T. Routti and J. V. Sandberg, "General Purpose Unfolding Program LOUHI78 with Linear and Nonlinear Regularizations." Helsinki Univ. of Technology, Report TKK-F-A359 (1978).

[2] J. D. Cossairt, D. W. Grove and M. A. Gerardi, "Measurements of Radiation Quality Factors Using a Recombination Chamber." Fermi National Accelerator Laboratory, Report TM-1248 (1984).

[3] American National Standards Institute, "American National Standard for Dosimetry - Personnel Dosimetry Performance - Criteria for Testing." Report No. N13.11 (New York, 1983).

[4] D. E. Hankins, S. G. Homann and J. Westermark, "Personnel Neutron Dosimetry Using Electrochemically Etched CR-39 Foils." Lawrence Livermore National Laboratory Report UCRL-53833 (1987).

[5] J. Llacer, C. A. Tobias, W. R. Holley and T. Kanai, "On-line Characterization of Heavy-Ion Beams with Semiconductor Detectors." Med. Phys. **11**, 266 (1984).

[6] H. Ing, "The Status of the Bubble-Damage Polymer Detector." Nucl. Tracks Radiat. Meas. **12**, 49 (1986); and private communication (1988).

[7] W. A. Cross, A. Arneja and J. L. Kim, "Neutron Energy and Angular Response of Electrochemically Etched CR-39 Dosemeters." Radiat. Prot. Dosim. **20**, 49 (1987).

FIGURE CAPTIONS

Fig. 1. Plan view of experimental setup at the LBL Bevalac Biomedical Facility.

Fig. 2. Charged particle spectra observed by the Berklet detector at three angles to the beam direction shown in Fig. 1.

Fig. 3. Spectrum obtained with neutron spectrometer measurements unfolded by the program LOUHI78 for location A.

Fig. 4. Spectrum of previous figure depicted as cumulative percentages of fluence and dose equivalent.

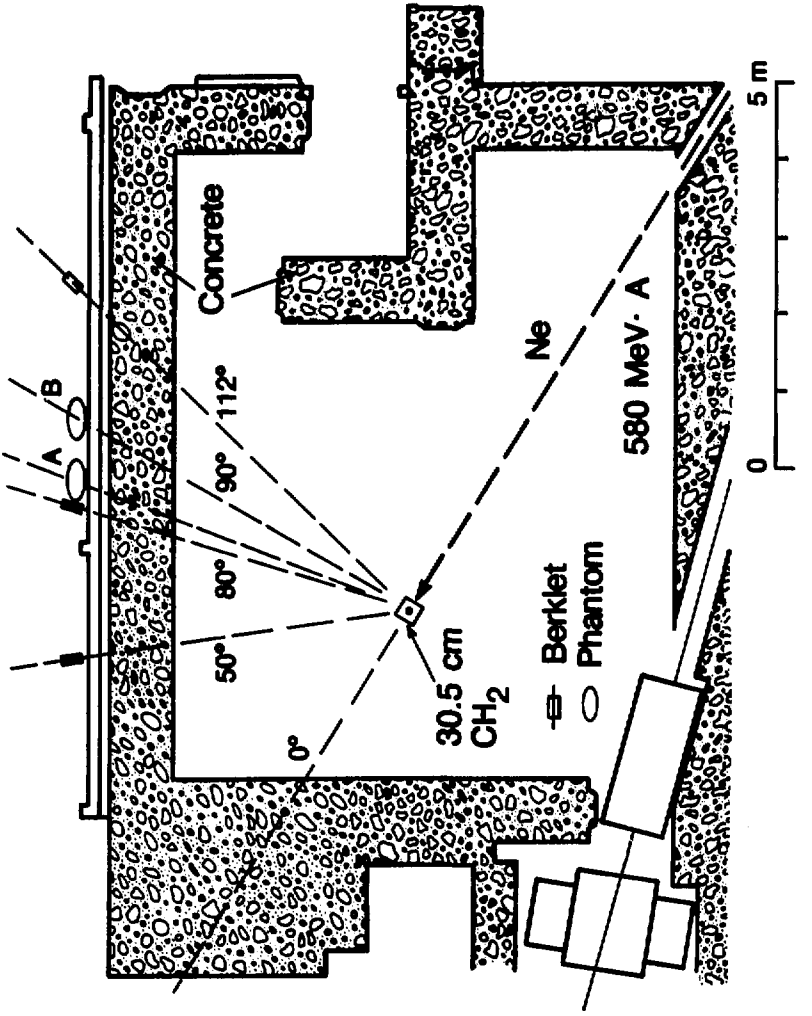

XBL 862-9568

Fig. 1

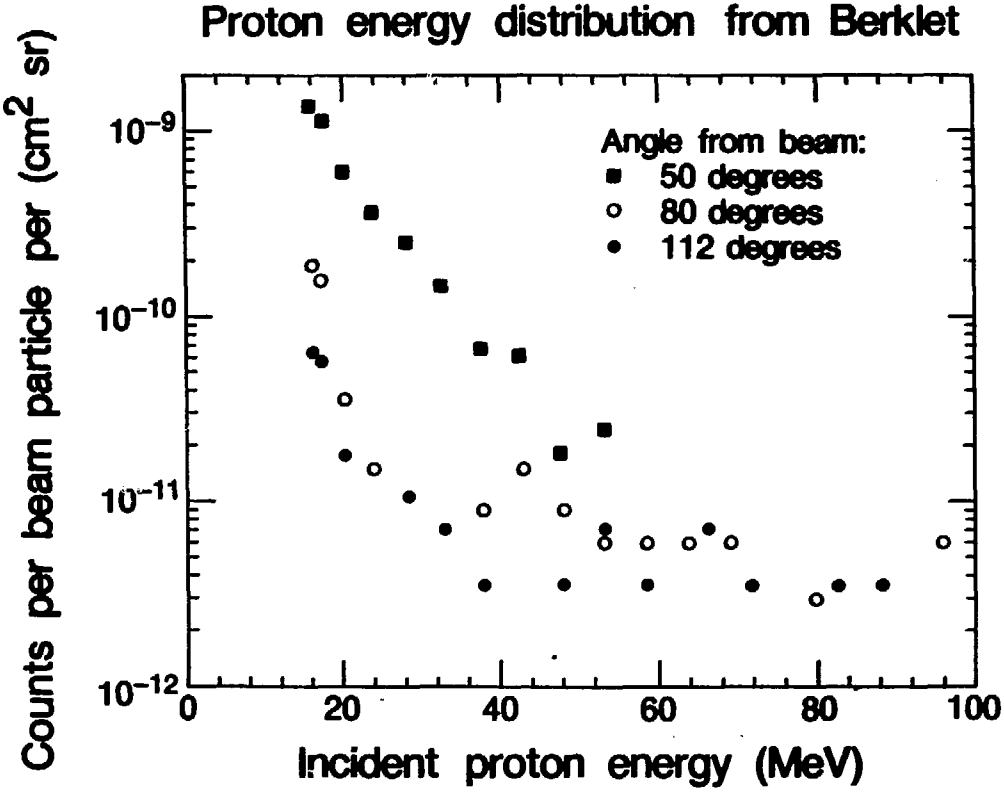

Fig. 2

XBL 862-9567

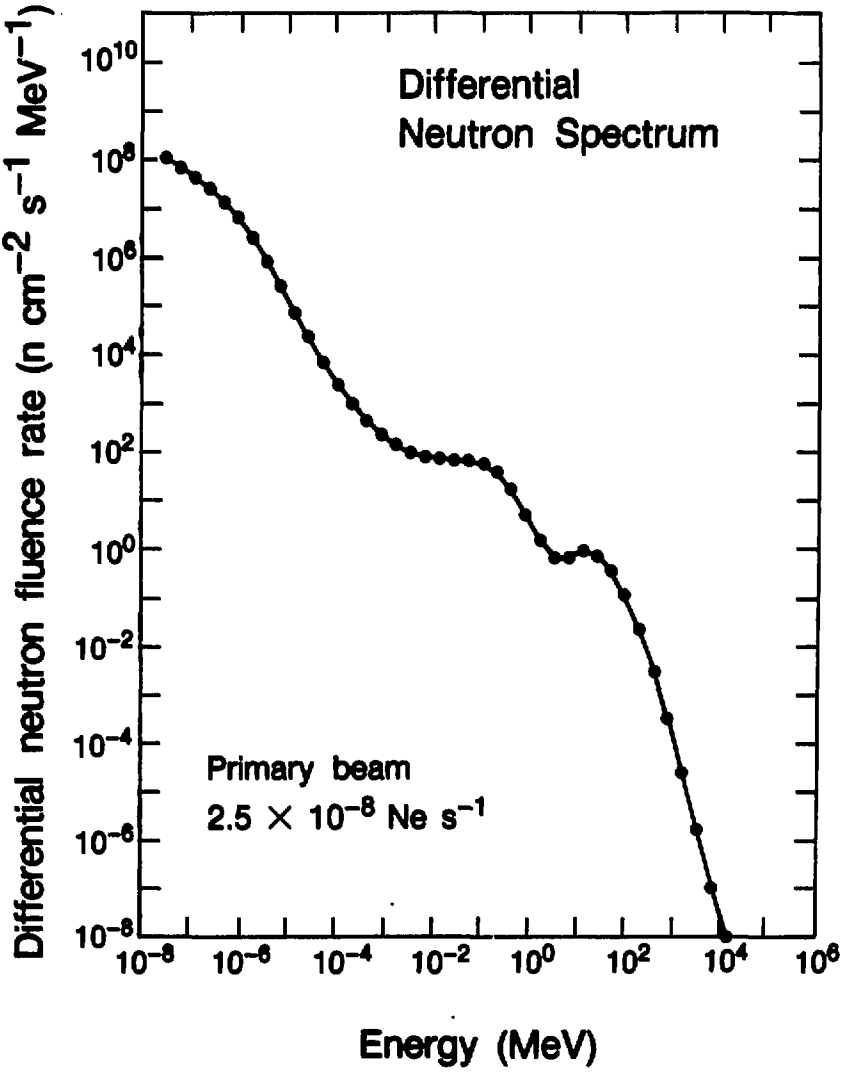

Fig. 3

XBL 862-9565

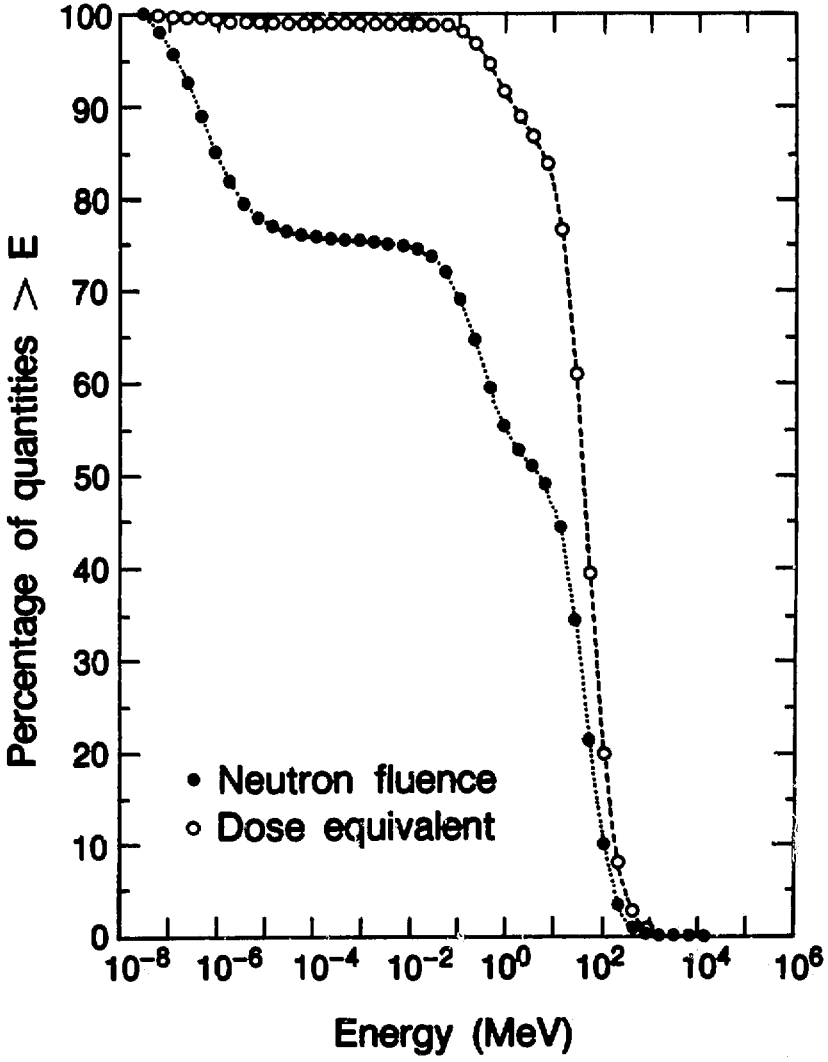

XBL 862-9506

Fig. 4